Global and Planetary Change 152 (2017) 38–50

Contents lists available at ScienceDirect

Global and Planetary Change

journal homepage: www.elsevier.com/locate/gloplacha

Invited research article

Late Burdigalian sea retreat from the North Alpine Foreland Basin: new magnetostratigraphic age constraints

K. Sant [a,*], U. Kirscher [a,b,c], B. Reichenbacher [d], M. Pippèrr [d], D. Jung [e], G. Doppler [f], W. Krijgsman [a]

[a] Paleomagnetic Laboratory Fort Hoofddijk, Department of Earth Sciences, Utrecht University, Budapestlaan 17, 3584, CD, Utrecht, The Netherlands
[b] Ludwig-Maximilians-University, Munich, Department of Earth and Environmental Sciences, Geophysics, Theresienstr 41, 80333 Munich, Germany
[c] Earth Dynamics Research Group, ARC Centre of Excellence for Core to Crust Fluid Systems (CCFS), The Institute for Geoscience Research (TIGeR), Department of Applied Geology, Curtin University, GPO Box U1987, WA 6845, Australia
[d] Ludwig-Maximilians-University, Munich, Department of Earth and Environmental Sciences, Paleontology and Geobiology, Richard-Wagner-Str. 10, 80333 Munich, Germany
[e] Bavarian Environmental Agency, Hans-Högn-Str. 12, 95030 Hof, Saale, Germany
[f] Bavarian Environmental Agency, Haunstetter Str. 1 12, 86161 Augsburg, Germany

ARTICLE INFO

Article history:
Received 4 February 2016
Received in revised form 18 November 2016
Accepted 9 February 2017
Available online 20 February 2017

Keywords:
S-German Molasse
Magnetostratigraphy
North Alpine Foreland Basin
Miocene
Paratethys

ABSTRACT

Accurate reconstruction of the final sea retreat from the North Alpine Foreland Basin (NAFB) during the Burdigalian (Early Miocene) is hampered by a lack of reliable age constraints. In this high resolution magnetostratigraphic study we try to solve a significant age bias for the onset of the Upper Freshwater Molasse (OSM) deposition in the neighboring S-German and Swiss Molasse Basins. We measured >550 samples from eleven drill cores covering the transition from marine to brackish to freshwater environments in the S-German Molasse Basin. Based on combined bio-, litho- and magnetostratigraphic constraints, the composite magnetostratigraphic pattern of these cores provides two reasonable age correlation options (model 1 and 2). In model 1, the base of the brackish succession lies within Chron C5Cr (~16.7–17.2 Ma), and the onset of OSM deposition has an age of ~16.5 Ma. Correlation model 2 suggests the transition to brackish conditions to be within C5Dr.1r (~17.7–17.5 Ma), and yields an age around 16.7 Ma for the shift to the OSM. Most importantly, both models confirm a much younger age for the OSM base in the study area than previously suggested. Our results demonstrate a possible coincidence of the last transgressive phase (Kirchberg Fm) with the Miocene Climatic Optimum (model 1), or with the onset of this global warming event (model 2). In contrast, the final retreat of the sea from the study area is apparently not controlled by climate change.

1. Introduction

The North Alpine Foreland Basin (NAFB) formed during the Eocene as a result of gravitational loading by the advancing Alpine orogenic wedge (e.g., Sissingh, 1997; Hinsch, 2008). The paleogeographic and sedimentary evolution of the NAFB is closely related to uplift and erosion caused by Alpine tectonics and relative sea-level changes (e.g., Lemcke, 1988; Kuhlemann and Kempf, 2002). The Molasse Basin largely covers the area of the NAFB and belongs to the biogeographic provinces of the Western and Central Paratethys Seas (Fig. 1). It extends from Lake Geneva in the west via northern Switzerland and southern Germany to Lower Austria in the east. The oldest Molasse sediments date from the Late Eocene/Early Oligocene, while the youngest deposits are Late Miocene in age (e.g., Schlunegger et al., 1996; Doppler et al., 2005; Grunert et al., 2015). The Molasse sediments largely originate from erosional debris of the uplifting Alps, with lesser amounts of material deriving from sources to the North and axial and radial directions of sediment transport respectively (e.g., Lemcke, 1988; Kuhlemann and Kempf, 2002). Sedimentary thicknesses range from a few tens of meters in the distal areas to >5000 m nearby the Alps (e.g., Lemcke, 1988).

Key features of the Oligocene to Miocene infill are two transgressive-regressive megacycles, each consisting of a succession of marine, brackish and freshwater sediments (Bachmann and Müller, 1992; Schlunegger et al., 1996; Berger et al., 2005a,b; Grunert et al., 2015). Six main lithostratigraphic groups have been established in the S-German Molasse Basin, comprising (from bottom to top) the Lower Marine Molasse, the Lower Brackish Molasse, the Lower Freshwater Molasse, the Upper Marine Molasse, the Upper Brackish Molasse, and the Upper Freshwater Molasse. Flora and fauna of the semi-enclosed Paratethys environments contain many endemic elements, while index species of the Tethys are often absent. This makes biostratigraphic correlation to the global ocean record difficult and resulted in the development of regional stratigraphic schemes for the Paratethys domains (e.g., Piller et al., 2007; Hilgen et al., 2012). In addition, the sequence stratigraphy of the Molasse Basin and possible correlations to global

* Corresponding author.
E-mail address: k.sant@uu.nl (K. Sant).

http://dx.doi.org/10.1016/j.gloplacha.2017.02.002
0921-8181/

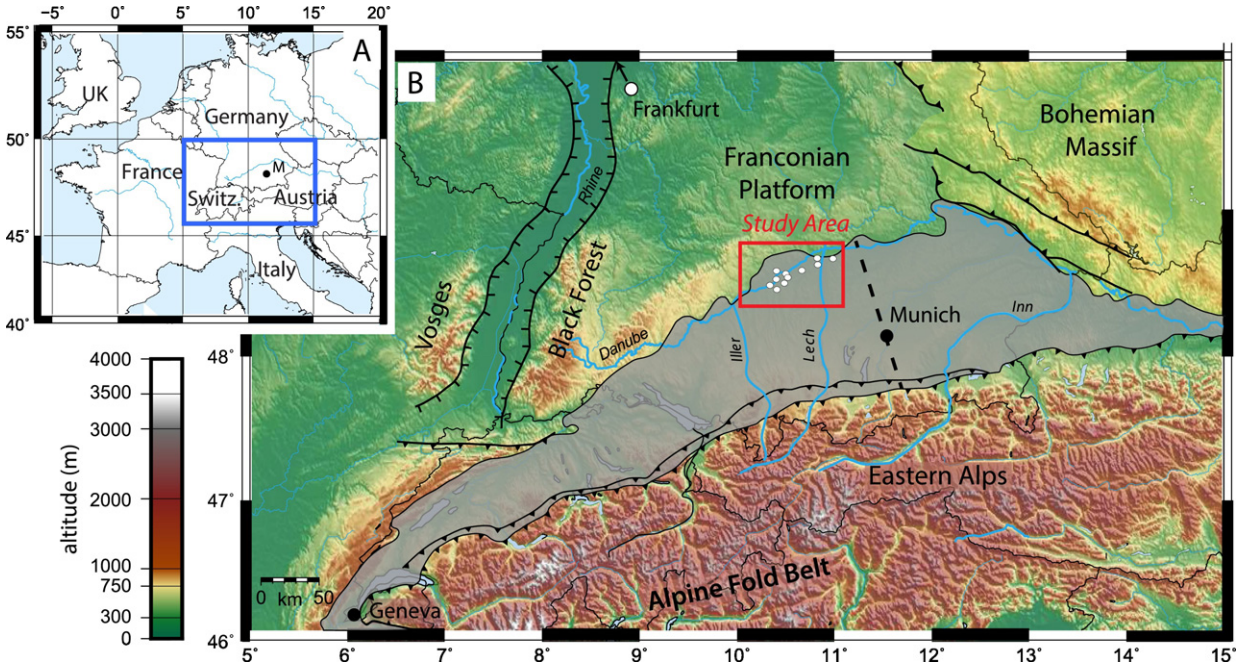

Fig. 1. Geographic location of the study area indicated in a topographic map of the North Alpine region (B) in Europe (A). Schematic outline of the Molasse Basin (in gray) modified after Jin et al. (1995). Coordinates of drill cores (white dots) are stated in Table 1. The dashed line through Munich indicates the boundary between the Western and Central Paratethys regions (Senes, 1973).

sea level changes were discussed intensively (e.g., Jin et al., 1995; Zweigel et al., 1998; Hinsch, 2008; Frieling et al., 2009; Grunert et al., 2013). As a result, most of the current regional time scales rely on biostratigraphy combined with basin sequence stratigraphy and 3rd order global sea level variations (sensu Hardenbol et al., 1998), whereas absolute age constraints on the sequence boundaries are often absent.

In this paper, we will focus on part of the second transgressive-regressive megacycle developing in the NAFB from the Early Miocene (late Aquitanian-to-Burdigalian) to the Late Miocene (Tortonian). The shift from marine conditions, represented by the Upper Marine Molasse (OMM),[1] via mainly brackish environments termed the Upper Brackish Molasse (OBM), to fluvial and lacustrine depositional settings recorded by the Upper Freshwater Molasse (OSM), marks an important change in Paratethys paleogeography. At the onset of OSM sedimentation, the marine connection between the NAFB and the western Mediterranean via the Rhône Basin was restricted or closed (Sissingh, 2001). Uplift between the Eastern Alps and Bohemian Massif separated the western NAFB (Switzerland and S-Germany) from the rest of the Central Paratethys (Kuhlemann and Kempf, 2002) (Fig. 1).

A detailed understanding of the final sea retreat from the central and northern NAFB during the Burdigalian, however, is hampered by an age bias (up to 0.7 Myr) for the onset of freshwater deposition (OSM) in the S-German and Swiss Molasse Basins. According to Abdul Aziz et al. (2010), the base of the OSM in the central Molasse Basin in S-Germany is >17.5 Ma based on correlation of magnetostratigraphy, small mammal biostratigraphy and Ar/Ar ages of two bentonites. In contrast, it was defined to be at around 16.8 Ma in the southern Molasse Basin in Switzerland, based on mammal stratigraphy, magnetostratigraphy and U/Pb ages of bentonites (Kälin and Kempf, 2009). Some diachrony can be expected, even in neighboring regions such as the Swiss and S-German Molasse Basin, but a difference of about 0.7 Myr is difficult to understand, mainly because the small mammal assemblages at the base of the OSM are similar (MN 4/MN 5 transition) in both regions. Furthermore, it is unlikely that the sea retreat would occur much earlier in the central part than in the alluvial fan-dominated proximal part of the basin.

Recently, Reichenbacher et al. (2013) tried to resolve this age controversy. They performed a magneto-litho-biostratigraphic study on four sections and three boreholes of the Swiss and S-German Molasse Basins and suggested that the base of the OSM is ~16.7 Ma in S-Germany and ~16.5 Ma in Switzerland (Fig. 2). The new data and revised correlation largely solve the age difference between the Swiss and German regions. However, the magnetostratigraphy of the S-German cores was based on a rather low sampling resolution with several polarity intervals only based on 1 or 2 samples.

The objectives of this study are to refine the chronostratigraphy of the Upper Brackish to Upper Freshwater Molasses by applying high-resolution magnetostratigraphy and to test if the new age model of Reichenbacher et al. (2013) can be supported. Our new database comprises >550 samples from eleven drill cores covering the marine to brackish to freshwater transition in the western S-German Molasse basin (Fig. 1, Table 1). The new age constraints will allow better correlation between the S-German and Swiss Molasse Basins and improve understanding of the final sea retreat from the Molasse Basin during the Early Miocene.

2. Geological setting

2.1. Overview

The OMM in the S-German Molasse Basin is dominated by glauconitic sands and marls, and is generally rich in foraminifers and other marine fossils. Biostratigraphy is based mainly on mollusks and benthic foraminifers, and correlation to global biostratigraphy based on planktonic foraminifers and nannoplankton is limited due to rarity of index fossils (e.g., Steininger et al., 1976; Cicha et al., 1998; Pippèrr, 2011). In the regional Central Paratethys stratigraphic framework, the OMM consists of an Eggenburgian and Ottnangian part; in the central S-German

[1] To avoid confusion with the classic German terminology, the German abbreviations will be used for the lithostratigraphic units of the Molasse Basin, being the Obere Meeresmolasse (OMM), Obere Brackwassermolasse (OBM) and Obere Süβwassermolasse (OSM).

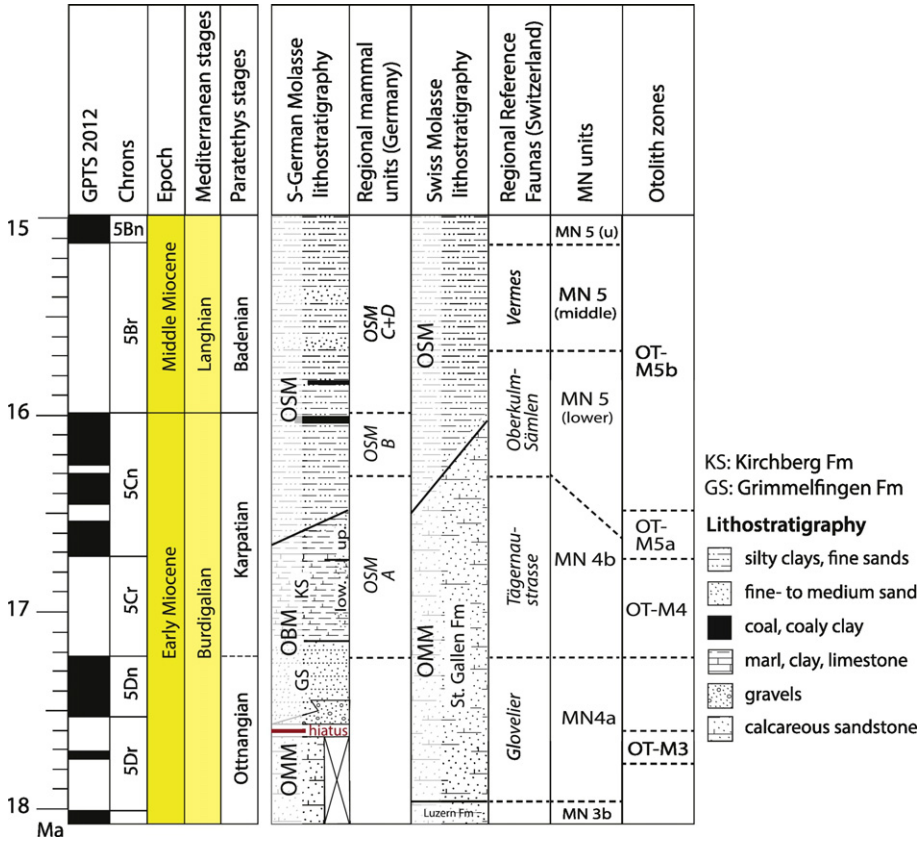

Fig. 2. Chrono-, litho- and biostratigraphic framework for the study area in the S-German Molasse Basin and for the central and northern (distal) part of the Swiss Molasse Basin. Time scales are according to Hilgen et al. (2012). Generalized stratigraphy of the sub-basin, regional faunal zones and mammal (MN) units are after Reichenbacher et al. (2013); lower boundary of Kirchberg Fm according to Pippèrr and Reichenbacher (2017). Regional otolith zonation after Reichenbacher (1999). Dashed lines indicate boundary positions that are poorly constrained by independent age data. OMM = Upper Marine Molasse, OBM = Upper Brackish Molasse, and OSM = Upper Freshwater Molasse.

Molasse Basin the thickness is usually up to 200 m (Doppler et al., 2005). Biostratigraphically, the Ottnangian OMM can be subdivided into a lower and middle Ottnangian segment, with the lower Ottnangian represented by fully marine facies, and the middle Ottnangian characterized by restricted marine environments (e.g., Wenger, 1987; Pippèrr et al., 2016).

A late Burdigalian ('late Ottnangian') retreat of the OMM sea took place in the S-German Molasse Basin, while the OMM sea persisted to the east and also in the Swiss Molasse Basin to the west (e.g., Lemcke, 1988). Most likely as a result of this regression, pedogenesis occurred at the basin margins and calcareous nodules known as "Albstein" formed in the uppermost OMM-sediments of the western S-German Molasse Basin (e.g., Lemcke et al., 1953; Doppler et al., 2005). In addition, the large "Graupensandrinne", an up to 80 m deep and up to 13 km wide channel like depression, developed (e.g., Moos, 1926; Kiderlen, 1931; Reichenbacher et al., 1998). The ENE-WSW-oriented depression was located along the northwestern margin of the S-German Molasse Basin and eroded into the underlying strata of the OMM and parts of the Lower Freshwater Molasse.

The Graupensand channel was filled by up to 50 m thick sands and gravels, termed the Grimmelfingen Schichten (GS) (Lemcke, 1988), or Grimmelfingen Formation (Reichenbacher et al., 2013). This siliciclastic succession reveals occasionally brackish bivalves (e.g., *Rzehakia*), shark teeth, small mammal teeth, and freshwater gastropods (e.g., Reichenbacher et al., 1998, Sach and Heizmann, 2001). Most of the sands and gravels have been deposited by the Graupensand-River, as evidenced by typical black chert gravels that have their source in the Frankenwald of the Bohemian Massiv (Lemcke, 1985, Fig. 1). In continuous profiles, the uppermost meters of the GS are characterized by finer grained sediments like fine sands and silts, at places with abundant *Rzehakia* and the gastropod *Viviparus suevicus*, representing a low energy fluviatile to estuarine facies. This typical facies of the GS is termed "Graupensand-Deckschichten" (GD) (Doppler, 1989; Pippèrr and Reichenbacher, 2017).

As a result of a short marine ingression, probably from the Swiss Molasse Sea, the up to 10 m thick marls and silts of the Kirchberg Fm (=Kirchberger Schichten = Kirchberg Beds = KS) filled up the Graupensand channel and usually overly the GS (Kiderlen, 1931; Büchi and Schlanke, 1977; Lemcke, 1988; Pippèrr and Reichenbacher, 2017). The lithostratigraphic concept of the KS, the type locality of which is Illerkirchberg, was initially based on Kranz (1904), Schlickum (1963) and Reichenbacher (1989). Recently, Pippèrr and Reichenbacher (2017) presented a revised diagnosis for this formation by newly drawing its lower boundary, which we have adopted for our study. Accordingly, the base of the KS coincides with the first occurrence of fossiliferous marly sediments with a rich and often well-preserved macrofauna, mainly composed of marine-euryhaline bivalves (e.g.,

Table 1
GPS coordinates (WGS84, decimal degrees) of the studied drill core localities.

Core name	Latitude	Longitude
Hamlar-1 (HA)	48.688818	10.83286
Druisheim (DR)	48.637613	10.838262
Gempfing (GE)	48.684979	10.994146
Lauingen (LA)	48.588575	10.413759
Gundremmingen (GU)	48.522564	10.411664
Holzheim (HH)	48.536755	10.529678
Dillingen (DI)	48.565518	10.50894
Buttenwiesen (BU)	48.592383	10.674599
Burgau (BUR)	48.441168	10.417449
Offingen (OF)	48.474453	10.346205
Glött (GL)	48.491368	10.494236

Cerastoderma sociale) as well as brackish bivalves and gastropods (*Mytilopsis amygdaloides*, *M. clavaeformis*, *Ctyrokya conoidea*, *Nematurella*).

This new lithostratigraphic concept securely allows identifying the basis of the KS in boreholes and sections. The subdivision into the lower and upper KS is based on characteristic assemblages of macro- and microfossils. The marine-euryhaline and brackish species of the above-mentioned bivalves and gastropods are largely restricted to the lower KS. The upper KS is recognizable based on abundant opercula of the gastropod *Bithynia* that co-occur with the ostracod *Mediocypris candonaeformis*, otoliths of *Gobius* and *Eleogobius* and, more rarely, *Dapalis* (see Reichenbacher et al., 2013; Gierl and Reichenbacher, 2015; Pippèrr and Reichenbacher, 2017 for further information).

The Albstein, Grimmelfingen Fm and Kirchberg Fm in the western S-German Molasse Basin together form the lithostratigraphic group of the Upper Brackish Molasse (OBM) (Doppler et al., 2005, Fig. 2). The Kirchberg Fm and Albstein deposits are concordantly or discordantly overlain by the limnic or fluvial sediments of the OSM (e.g., Abdul Aziz et al., 2010; Reichenbacher et al., 2013). Both in the German and Swiss Molasse Basins, the lower part of the OSM sediments are clayey fine-sands and silts with occasionally coaly intervals and palaeosoils, followed by sands (e.g., Doppler, 1989; Prieto et al., 2009). The stratigraphy of the OSM is mainly based on small mammal biostratigraphy and magnetostratigraphy (e.g., Kälin and Kempf, 2009; Abdul Aziz et al., 2010; Reichenbacher et al., 2013), and also otoliths can be used in the lower part (e.g., Reichenbacher, 1999; Jost et al., 2015).

2.2. The studied boreholes

The drill cores studied here are derived from the western S-German Molasse Basin from 11 boreholes (Fig. 1) that were drilled under the auspices of the Bavarian Environmental Agency (Bayerisches Landesamt für Umwelt, LfU Bayern), mostly as research drillings (Forschungsbohrung, FB) between 2010 and 2014 (Fig. 1, Table 1). Most of them were located in the area of the former Graupensand channel, only the drillings of Burgau and Glött were situated to the south. With the exception of the cores Burgau and Glött, all sampled cores cover the upper part of the S-German Molasse, namely the OSM and OBM down to the basal unconformity caused by the Graupensand channel incision (Fig. 2, Suppl. B). In some drill cores the characteristic lithofacies of the GD is partially or completely missing (e.g., Buttenwiesen) and therefore a hiatus can be assumed nearby the base of the KS.

The OMM sediments of Burgau and Glött consist of carbonate rich glauconitic sands and silty to sandy marls (no Grimmelfingen Formation (GS) is developed because Burgau and Glött are placed outside the Graupensand channel). In the other cores, the deposits of the GS are largely comprised of carbonate-poor to -free, coarse- to fine-grained, sometimes gravelly sands; fossils are rare and mainly represented by the bivalve *Rzehakia* and freshwater gastropods. In most cases, the mica-rich sands contain few, if any, small-sized glauconite grains (probably reworked). In most cores, the uppermost part of the GS consists of fine-grained deposits (GD) including mainly carbonate-poor to -free, in some places also carbonate-rich, silty to fine-sandy sediments. The KS is characterized by fossiliferous clay-rich to silty marls, in places accompanied by fossiliferous marly limestones and calcareous, fine-grained sands; no *Rzehakia* is present. The deposits of the OSM mostly include silt, sands and a few marly layers with rare fossils. All boreholes, fossil content and biostratigraphic data have been described in detail in Pippèrr and Reichenbacher (2017) and we refer the reader to this study for details.

3. Material and methods

We conducted a detailed sampling of the OBM in all cores, except Burgau where OBM is not present (see Supplementary material B for details). Only in the cores Burgau and Glött a part of the OMM could be sampled (because these drillings lie outside the Graupensand channel). The cores are logged as LfU-FB Burgau 1, LfU-FB Glött 1, LfU-FB Dillingen 1, LfU-FB Gundremmingen 1, LfU-FB Holzheim 1, Gempfing W4, LfU-FB Druisheim 1, LfU-FB Lauingen, LfU-FB Hamlar 1, LfU-FB Buttenwiesen 1 and LfU-FB Offingen 1. All cores are stored in the Bavarian Environmental Agency's archive in Hof (Germany).

Standard paleomagnetic cores with a horizontal orientation were obtained with an electric drill. In fine-grained intervals the sampling resolution was approximately 1 m or lower, while in coarser grained intervals it reached 5 m. In the cores Hamlar-1, Druisheim and Gempfing, which were also studied by Reichenbacher et al. (2013), the sampling was expanded to non-sampled intervals and, if lithology allowed, the sampling resolution was increased up to 0.5 m around potential reversals. All sampling positions are indicated in detail in the Supplementary material B.

As mentioned above, the studied sediments usually show a typical lithofacies and contain characteristic assemblages of macro- and microfossils that allow identifying the OMM, Albstein, GS, KS and OSM, and even the lower and upper KS in the boreholes. Furthermore, the KS can be assigned to otolith zone OT-M4 (*Dapalis formosus* taxon-range zone) and the GD in Offingen has yielded a rodent tooth of *Megacricetodon*, which indicates an age not older than small mammal zone MN 4b (for details see Pippèrr and Reichenbacher, 2017).

Prior to the demagnetization experiments, the magnetic susceptibility per mass was determined of all samples using an Agico MFK1 Kappabridge at field strength of 200 A/m and a frequency of 976 Hz. For determination of the paleomagnetic directions, a one inch long sample of each specimen was demagnetized using alternating field (AF) and thermal cleaning techniques at the Universities of Munich and Utrecht. A preliminary set of 129 samples was stepwise demagnetized with alternating fields using the homemade automated system of the University of Munich within a shielded room (Wack and Gilder, 2012). Additionally, 192 samples were similarly cleaned by the automated system housed in the paleomagnetic laboratory 'Fort Hoofddijk' at Utrecht University. In both cases peak fields of 90 mT were applied. Another 262 samples were heated stepwise up to 680 °C using a magnetically shielded ASC thermal demagnetizer at the University of Utrecht. In all cases the magnetization was measured in three components at each demagnetization step with a 2G Enterprises DC Squid magnetometer (noise level: $3 \cdot 10^{-12}$ Am^2).

Out of all AF demagnetized samples, a representative fraction (26 samples) was furthermore used for applying a stepwise Isothermal Remanent Magnetization (IRM) using again the automated system of the University of Utrecht. 60 IRM steps were imparted with a peak field of 700 mT. Small parts (~200 mg) of representative specimen of each drill core, lithology and stratigraphic unit were additionally used for thermomagnetic experiments using a VFTB (Krása et al., 2007) at the University of Munich (bias field of ~180 mT) and a modified horizontal translation type Curie balance (noise level $5 \cdot 10^{-9}$ Am^2) at the University of Utrecht. Care has been taken to use samples from all different lithologies for rock magnetic analysis.

Because of the undefined azimuthal orientation of the drill cores only the vertical components (inclinations) can be used for further analysis. For analyzing the AF and thermal demagnetization data, linear segments at the orthogonal projection of the data (Zijderveld, 1967) were used and quantified using a least square method (Kirschvink, 1980) on at least four consecutive demagnetization steps. The uncertainty of the fits was calculated using common paleomagnetic statistics (Fisher, 1953). The acquisition data of the IRM was interpreted using the component analysis of Heslop et al. (2002) and Kruiver et al. (2001). The number of components has been constrained to two or three depending on the level of distinction between them.

4. Results

4.1. Rock magnetic properties

Regarding each of the different drill cores, the rock magnetic results can be interpreted as being caused by a heterogeneous mixture of magnetic particles, which occur in varying amounts and proportions. The magnetic intensity is generally rather low and the thermomagnetic and hysteresis data are dominated by a paramagnetic response to the applied field (Fig. 3, Table 2 and Suppl. A). After correcting the signal for the paramagnetic contribution, the most striking feature in the thermomagnetic diagrams is the formation of a new magnetic mineral between 400 and 600 °C (Fig. 3d,f), and between 500 and 650 °C (Fig. 3a,e). This might be related to the conversion of pyrite and/or clay minerals into magnetite (Hirt and Gerhring, 1991; Passier et al., 2001). Furthermore, the thermomagnetic experiments indicate unblocking temperatures in the range of 550–600 °C (Fig. 3c, d) and in the range between 600 and 700 °C (Fig. 3a, b, e, f). Additionally, there is some slight indication of a low temperature phase (Fig. 3a, b, c, f).

The IRM acquisition results can be grouped basically in three end members (Fig. 3g). Group 1 is dominated by a low coercivity phase ($B_{1/2}$ between 20 and 30 mT, see Table 2 and Suppl. A) and saturation is reached quickly by 200 mT (e.g., sample BU-03). Group 2 is characterized by a medium coercivity phase ($B_{1/2}$ between 50 and 70 mT) and saturation is reached only after applying fields of ~400 mT. Finally, the last group 3 has only high coercivity phases ($B_{1/2}$ > 150 mT), where saturation is not reached at 700 mT (e.g., sample HH-43). Most samples yield mixtures of groups 1 and 3 (Suppl. A).

In summary, the magnetic signal of the sampled material is interpreted to be controlled by magnetite (group 1) and hematite (group 3). Only very rarely indications of greigite (group 2) occur. The occurrence of different magnetic carriers is related to the sedimentary environment and/or source area, but a more detailed rock magnetic analysis would be necessary to verify this. We point out that a straightforward correlation of quality of magnetic signal and lithology cannot be made. Fine grained clay samples and coarse grained sandy samples both gave high and low quality magnetic results. Ultimately, hematite, magnetite and greigite samples do not show systematic different directional behavior, which indicates that all minerals can reflect a primary magnetic signal. Probably the formation of greigite is related to more anoxic conditions within the sediment and the formation of hematite to paleosoils, which are mainly present in the Upper Freshwater Molasse.

The specific magnetic susceptibilities show different patterns per drill core. In most cases, the average susceptibility is higher in the OSM than in the underlying beds. No clear correlation between abrupt shifts in lithology/hiatuses and susceptibility is visible (Suppl. B).

Table 2
Parameters of the fitted IRM data for representative samples after using the component analysis of Heslop et al. (2002) and Kruiver et al. (2001). SIRM = Saturation Isothermal Remanent Magnetization. $B_{1/2}$ = remanent coercivity force. DP = dispersion parameter. See Supplementary material A for graphs.

Sample	Comp.	SIRM [A/m]	$B_{1/2}$ [mT]	DP	IRM Contr.
HH-43	1	3.87E + 04	126	0.8	6
	2	1.15E + 05	228	0.16	20
	3	4.31E + 05	371.5	0.13	74
HH-82	1	1.59E + 04	27.5	0.6	3
	2	1.41E + 05	57.2	0.39	30
	3	3.13E + 05	854	0.33	67
HA-38	1	9.83E + 03	22.7	0.64	8
	2	4.57E + 04	62.7	0.27	37
	3	6.65E + 04	103.5	0.54	54
BU-03	1	2.17E + 04	24.9	0.56	18
	2	1.00E + 05	28	0.34	82
OF-33	1	1.55E + 04	53.3	0.51	1
	2	1.16E + 06	73.4	0.13	63
	3	6.81E + 05	77.8	0.34	37

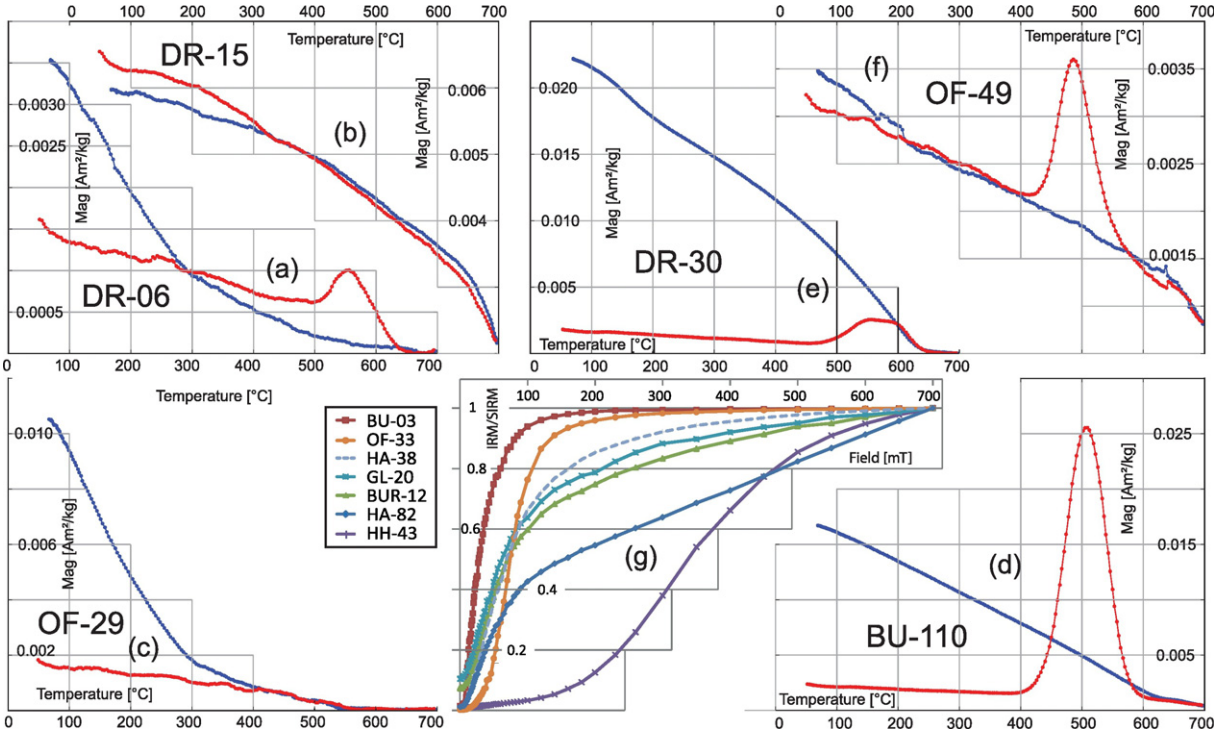

Fig. 3. Rock magnetic results of representative samples from the Molasse cores: (a–f) Thermomagnetic curves where red (blue) indicates the heating (cooling) cycle; lithologies: DR-06 = clayey silt, DR-15 = orange-brown mottled silty clay, DR-30 = fine-sandy silt, OF-49 = silty fine-sand, OF-29 = organic rich silty clay, BU110 = silty fine-sand. (g) Representative examples of different trends after acquisition experiments of isothermal remanent magnetization (IRM, Kruiver et al., 2001); lithologies: BU-03 = marl, OF-33 = fine-sandy silt, HA-38 = carbonate-rich fine-sand, GL-20 = silty clay, BUR-12 = clayey silt, HA-82 = clayey silt, HH43 = silty clay. Magnetization is normalized according to Saturation IRM (SIRM) value, see Table 2 for details. (For interpretation of the references to color in this figure legend, the reader is referred to the web version of this article.)

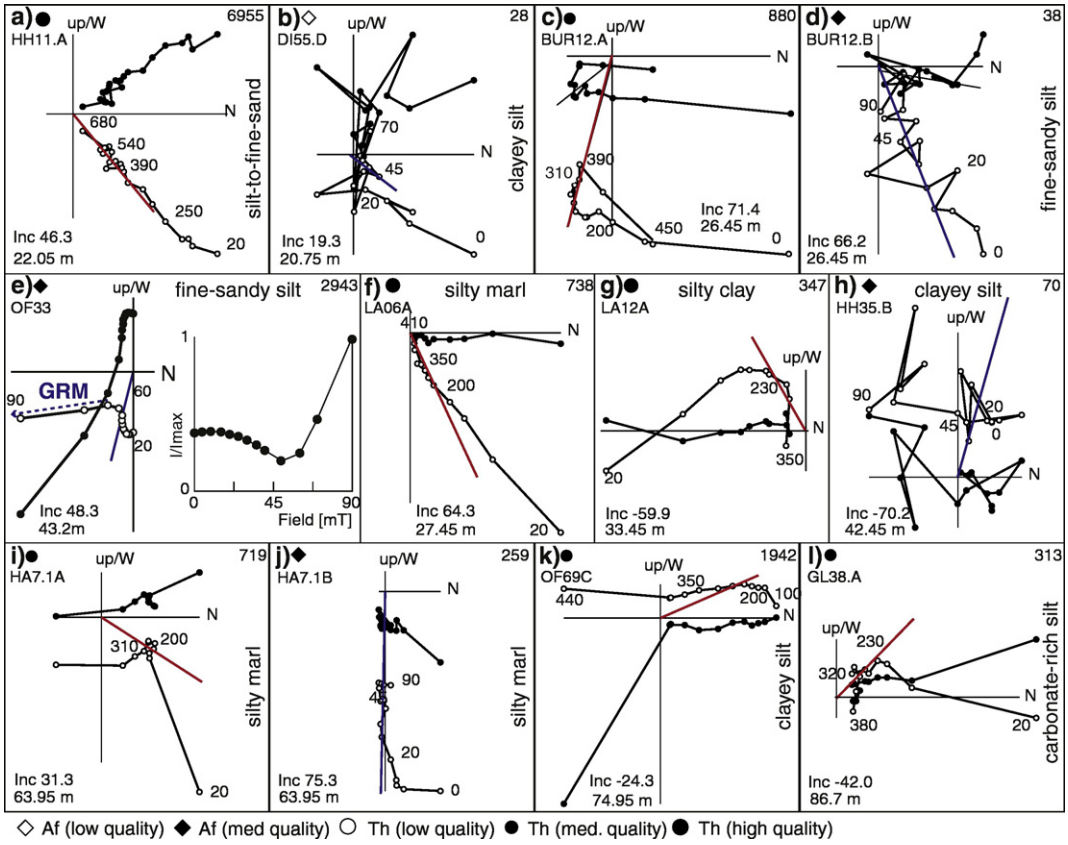

Fig. 4. Results of stepwise thermal (Th) and alternating field (Af) demagnetization experiments on orthogonal vector endpoint diagrams (Zijderveld, 1967) of representative samples from different lithological units of the Molasse cores. a–e = Upper Freshwater Molasse; f,g,i,j = Kirchberg Beds, h = Graupensand-Deckschichten = k: Grimmelfingen Beds; l = Albstein Fm. Open (closed) symbols indicate inclination (declination). Red (blue) lines to origin represent the best fit of principal component analysis (Kirschvink, 1980) after Th (Af) demagnetization. Stratigraphic sample depths in the profiles are indicated in the lower-left corners and intensities at 200 °C or 20 mT in μA/m are indicated in upper-right corners. An additional intensity graph in e) shows a sample with GRM. (For interpretation of the references to color in this figure legend, the reader is referred to the web version of this article.)

4.2. Demagnetization behavior

The demagnetization behavior of the samples is very heterogeneous throughout the different drill cores. Therefore the demagnetization results will be discussed for all localities together. The declination directions show a random distribution and the inclination values do generally not exceed 60° suggesting that the magnetic directions have not been aligned parallel to the axis of the drill core during mechanic drilling of the cores. After removal of a first viscous component at temperatures of 100 °C and fields of 20mT a low field/low temperature component is present in about 25% of the sampled material. After this first component, a characteristic component can be identified within the range 180 °C to 480 °C (in some cases up to 680°), and within the range 20 and 50–90 mT, respectively (Fig. 4). Generally, only one high temperature component is present even when the unblocking temperature reaches 680 °C. For a very limited number of samples (total of 6 samples) a gyro remanent magnetization (GRM, e.g., Stephenson and Snowball, 2001) is observed above ~50 mT (Fig. 4e). The mean magnetic intensities are very variable with maximum values between 40 and 9000 μA/m, and 35–7000 μA/m around 200 °C or 20 mT.

The demagnetization results have been grouped into a high, medium and low quality group (A–C) based on the demagnetization trends visible in the Zijderveld vector endpoint diagrams (Zijderveld, 1967). The high quality directions show a dominantly linear decay trend towards the origin, have a mean angular deviation (MAD) <8°, most of the times even below 5°. Their characteristic remanent magnetizations (ChRM's) are plotted in the temperature range 200 to ≥310 °C (e.g., Fig. 4a,f,g). Because of generally better constrained demagnetization results and higher stabilities, only TH samples are assigned to this high quality group, and thereby priority has been given to TH demagnetization results for interpreting the polarity patterns (Fig. 5). The medium quality data group B contains TH and AF samples that show a more scattered decay behavior than the high quality group, but still have an unambiguously defined polarity (e.g., Fig. 4c,d). Most of those samples do not decay completely towards the origin. The MAD for group B is mostly <21°; TH-samples generally have a MAD of 5–15°.The low quality group C contains demagnetization directions with a mean inclination below 10°, clustering diagrams without decay towards the origin, or directions plotted through <4 consecutive data points (e.g., Fig. 4b). Those MAD's are well above 10°. The stratigraphic positions of all samples are shown in the inclination graphs in Supplementary material B. Samples without any resultant vector are shown as crosses.

4.3. Polarity pattern

Plotting the inclination values from the demagnetization results in stratigraphic order allows to assign polarity patterns to all the different drill cores (Fig. 5, Suppl. B). We only consider individual polarity zones if they are based on a minimum of two successive levels of similar polarity with medium to high quality results of thermal demagnetization experiments. Isolated single polarity samples are indicated with a half bar, and uninterpretable intervals have been marked in gray (Fig. 5). These gray intervals are mostly related to the high sand content in the individual samples. Coarse-grained sediments are known for lower quality magnetic signals (e.g., Dupont-Nivet and Krijgsman, 2012). This

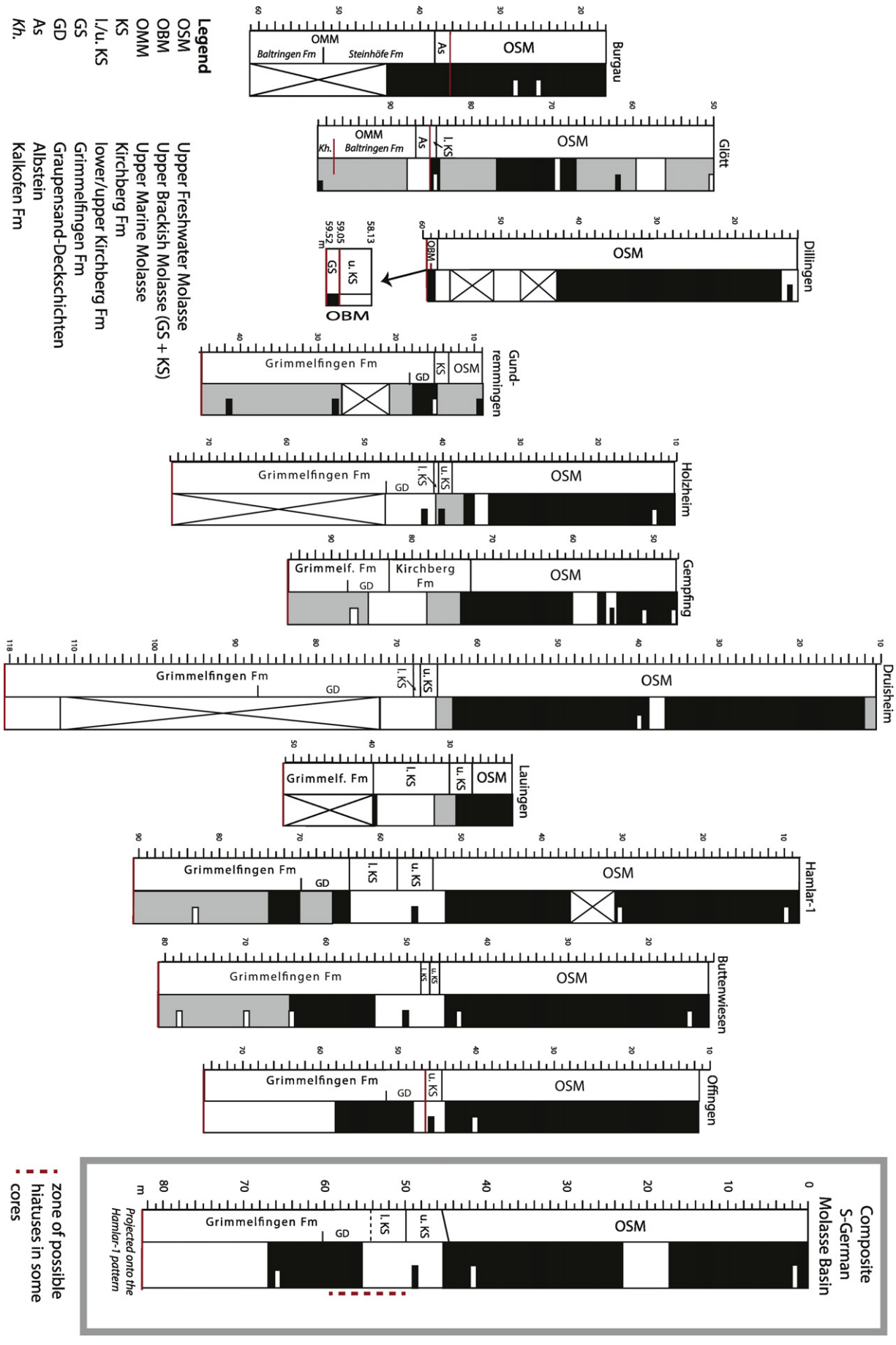
Legend
OSM Upper Freshwater Molasse
OBM Upper Brackish Molasse (GS + KS)
OMM Upper Marine Molasse
KS Kirchberg Fm
l./u. KS lower/upper Kirchberg Fm
GS Grimmelfingen Fm
GD Graupensand-Deckschichten
As Albstein
Kh. Kalkofen Fm
zone of possible hiatuses in some cores
Burgau
Glött
Dillingen
Gund-remmingen
Holzheim
Gempfing
Druisheim
Lauingen
Hamlar-1
Buttenwiesen
Offingen
Composite S-German Molasse Basin
Projected onto the Hamlar-1 pattern
OMM
Baltringen Fm
Steinhöfe Fm
OSM
OBM
Grimmelfingen Fm
Grimmelf. Fm
Kirchberg Fm
GD
KS
l. KS
u. KS
GS
As
Kh.
m

approach guarantees that individual polarity zones are not an artifact caused by lithological changes.

The polarity results of Reichenbacher et al. (2013) for the cores Druisheim, Hamlar-1 and Gempfing have been incorporated into the respective core interpretations after applying the same quality guidelines. For Hamlar-1, all high quality directions of Reichenbacher et al. (2013) and this study are consistent. Our new data filled in the former gap in between −66 and −56 m and expanded the pattern up to −10 m. For Druisheim, the inclination of the 2013 sample at level −40 m is opposite of the other directions in that zone. Since it only concerns one reversed sample it is marked by a half bar only (Fig. 5). Combining the 2013 and recent data in the upper part of Gempfing (−60 to −47 m) results in a complicated pattern, suggesting that perhaps the sedimentation in this zone is partly disturbed. One sign for this is the reworked foraminifers in the interval −56 to −54 m.

In most drill cores, the polarity patterns share several characteristics: (1) The Upper Brackish Molasse (OBM), consisting of the Kirchberg Formation (KS) and Grimmelfingen Formation [with uppermost facies GD], is characterized by a succession of reverse – normal – reverse polarity (especially in the cores with the most complete record). The reversed zone comprising the KS is present in all cores except for Gundremmingen; in some cores it includes the uppermost GS (GD). (2) The Upper Freshwater Molasse (OSM) is dominated by normal polarity. (3) A short reversed interval is present in the OSM in almost all cores. (4) The data obtained from the OMM in Glött and Burgau is not sufficient for a distinct interpretation.

The polarity profiles of Offingen, Buttenwiesen, Lauingen and Hamlar-1 are most complete and of highest quality for the OBM (GS, GD and KS). In Druisheim, Gempfing and Holzheim, the pattern in the OSM with one small reversed interval is best visible. Those seven cores serve as the basis for a composite polarity column for the S-German Molasse Basin (Fig. 5), which should be seen as a summary of the magnetostratigraphic data of the studied cores. Hamlar-1 was used as the basis to project the other polarity results onto, because the Kirchberg Beds seem well developed and can be assumed to be rather complete in this core (see also Reichenbacher et al., 2013; Pippèrr and Reichenbacher, 2017). However, the polarity of the GS-KS succession is probably disrupted in Hamlar-1, because the uppermost reverse part of GS (normally including the GD) is not present (Fig. 5). As several cores might be incomplete due to small hiatuses in this interval, it has been marked in the composite column. As a result, the exact position of the lowermost boundary of the KS within the reversed zone could not be determined exactly and has been marked with a dashed line. Special care has been taken to preserve the thickness ratios between the normal and reversed polarity intervals, so that the magnetostratigraphy in the composite column can be used for correlation to the Global Polarity Time Scale (GPTS).

5. Discussion

5.1. Correlation to the GPTS

Our magnetic polarity pattern of the composite column can be straightforwardly correlated to the late Burdigalian in the GPTS (Hilgen et al., 2012) when we assume more or less constant sediment accumulation rates. We realize that average sedimentation rates over a short amount of time are an oversimplification, especially in continental environments. However, we assume here that the preserved sediment thickness in the whole succession is a function of accommodation space, and therefore of subsidence (see discussion in Kirscher et al., 2016). With this assumption, the characteristic reversed – normal – reversed pattern within the OBM plus a thin reversed interval in the OSM would fit best to Chrons 5Cr – 5Cn.3n – 5Cn.2r, and to the small reversed Chron 5Cn.1r (Fig. 6, model 1). This magnetostratigraphic correlation of the Molasse Basin composite would indicate that the base of the OSM correlates roughly to the base of C5Cn.2n, resulting in an age of ~16.5 Ma (Fig. 6). In most cores, the entire Kirchberg Fm is of reversed polarity, except for Gempfing, Lauingen and Glött (Fig. 5). In the latter cores, the

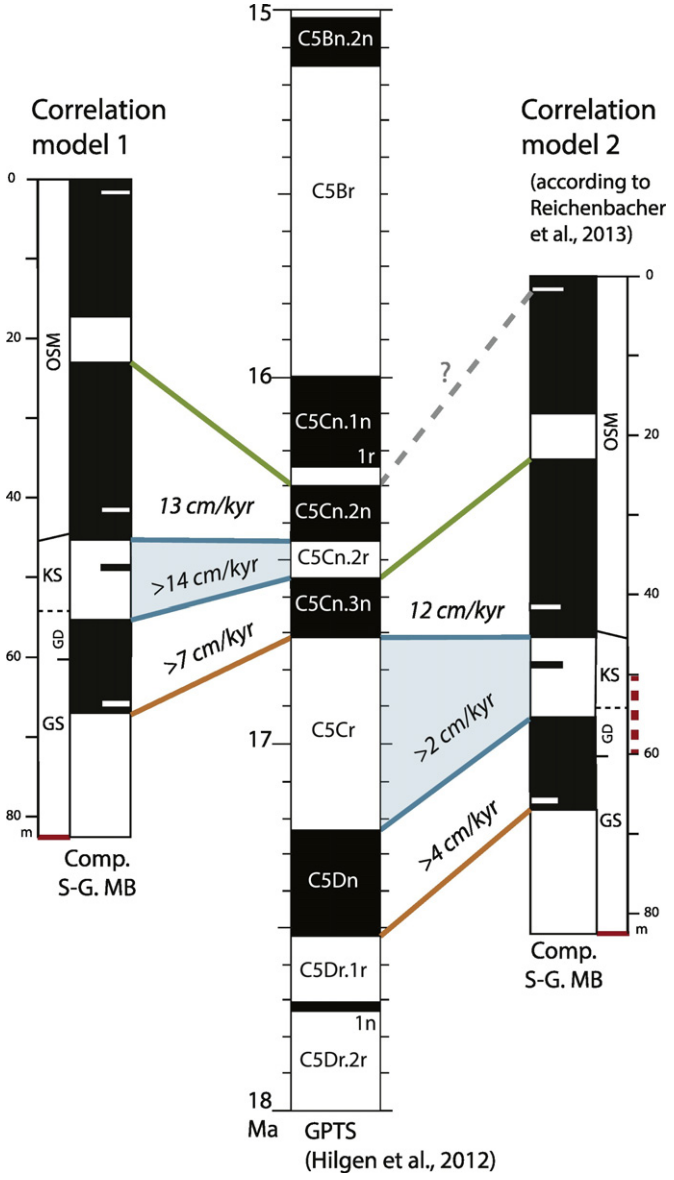

Fig. 6. Two favored correlations to the Global Polarity Time Scale (GPTS) of the composite S-German Molasse Basin polarity pattern (Comp. S-G. MB). Lines of the same color depict different correlations to the GPTS for the same reversal or polarity interval. The minimum, average accumulation rates are depicted in italics. See text and Fig. 5 for more details.

Fig. 5. Interpreted polarity patterns of the eleven drill cores of the study area. Individual sample positions are plotted in Supplementary material B. Black (white) zones indicate normal (reversed) polarity intervals, which are based on at least two levels with medium or high quality inclination results. Divergent or isolated polarity results based on only one level are marked with half bars. Intervals with low quality results are marked gray. Red horizontal lines in profiles, such as at the base of GS, mark proposed hiatuses. The composite S-German Molasse Basin profile summarizes the polarity patterns of the highest quality cores, notably Offingen, Buttenwiesen, Hamlar-1 and Lauingen for the OBM-OSM transition, and Druisheim, Gempfing and Holzheim for the OSM. Some hiatuses are inferred at the base of the lower KS, and therefore the exact position of the base of the Kirchberg Fm within the reversed zone is difficult to determine, and a dashed line is used. (For interpretation of the references to color in this figure legend, the reader is referred to the web version of this article.)

uppermost KS have 1–2 samples of normal polarity, indicating a slightly younger age for the base of the OSM. This is in agreement with paleomagnetic data of the Illerkirchberg section of the S-German Molasse Basin, which also has normal polarity in the uppermost KS (Reichenbacher et al., 2013). Alternatively, these normal polarities may be related to a short delay in acquisition of the magnetic remanence. The base of the OBM (base Grimmelfingen Fm) would be located in all cores in C5Cr, probably between 16.72 and 17.24 Ma. The fact that no core, except for Glött, has a long reversed polarity zone in the OSM suggests that C5Br was not reached and that the top of the OSM in our cores is thus older than 15.974 Ma (top C5Cn.1n).

A second, alternative correlation model places the base of the OSM to the lower part of C5Cn.3n at an age of 16.7 Ma (i.e. 200 kyr older than model 1). This proposed correlation supports the age model of Reichenbacher et al. (2013). In this model the characteristic reversed – normal – reversed pattern within the OBM would correlate from bottom to top to C5Dr.1r – C5Dn – C5Cr (see Fig. 6, model 2). In this case, the base of the OBM (GS) would be constrained between 17.7 and 17.5 Ma. This option would require the assumption of one or several hiatuses and/or severe changes in accumulation rate in the OBM in order to fit the short reversed zone in the Kirchberg Fm to the long reversed C5Cr (Fig. 6). However, multiple variations of sedimentation rates and presence of hiatuses are likely given the highly dynamic brackish-estuarine-lacustrine environments of the OBM (see also Kempf et al., 1999). The model further implies that the stratigraphic interval corresponding to C5Cn.1r in the OSM has not been clearly resolved in the majority of the cores, or that this level was not reached yet. Nevertheless, most cores contain one or two isolated reversed samples in the uppermost OSM.

Both correlation models are in agreement with previous magnetostratigraphic results of several OSM sections that belong to younger mammal and otolith zones than the successions of this study, such as the Ichenhausen, Untereichen-Altenstadt and Pfyffrüti sections (Abdul Aziz et al., 2010), that were correlated to C5Br (Reichenbacher et al., 2013). In addition, the correlations appear not to be in conflict with the previously established age of 17.8 ± 0.3 Ma for the base of the middle Ottnangian (the upper segment of the OMM, present in Burgau and Glött in Fig. 5). This age was determined by a combination of lithostratigraphy, small mammal stratigraphy (mammal unit MN 4a) and Sr-isotope data based on otoliths (Pippèrr et al., 2007).

One curiosity is that model 1 would require a completely new interpretation of the evolutionary lineage of the hamster *Megacricetodon*, which is the main index fossil for MN 4 and MN 5. The duration for the size increase in the teeth of *Megacricetodon* would become significantly shorter than previously assumed, namely 0.1 Myr according to model 1 vs. 0.4 Myr according to Reichenbacher et al. (2013: Fig. 13). As the *Megacricetodon*-lineage is constrained by bio-, litho- and magnetostratigraphy in the Swiss, S-German and Austrian Molasse Basin, many previous correlations would become invalid in the case of model 1 (e.g., Daxner-Höck, 1998; Abdul Aziz et al., 2008, 2010; Kälin and Kempf, 2009; Reichenbacher et al., 2013, Fig. 9).

Our new magnetostratigraphic results illustrate that the older correlation option of the base of the OSM according to Abdul Aziz et al. (2010) is very unlikely. These authors placed the base of the OSM in the S-German Molasse Basin to the base of the normal Chron C5Dn around 17.5 Ma. It is not possible to correlate the three normal polarity intervals in our S-German Molasse composite to the two normal chrons in the remainder of the Ottnangian interval (17.2–18 Ma) of the GPTS without inferring huge hiatuses, large accumulation rate changes and/or ignoring parts of the polarity pattern (Fig. 6). Moreover, this correlation would contradict previous age constraints for the lower Ottnangian OMM deposits (~18 Ma, Grunert et al., 2010, 2012) and the base of the middle Ottnangian sediments (17.8 ± 0.3 Ma, Pippèrr et al., 2007), because only about 0.3 Myr would be left for the middle Ottnangian, the incision of the Graupensand channel and the sedimentation of the OBM. Therefore, correlation model 1 and 2 provide the most likely time constraints for the studied interval.

5.2. Accumulation rates

The variety of lithologies together with the different positions of the cores in the basin already indicates that the accumulation rates are not constant between the different cores as well as within the drill cores. As stated before, we realize that average accumulation rates are an oversimplification, especially in continental environments. Nevertheless, we consider them useful to illustrate the differences between age model 1 and 2. The average accumulation rates were calculated with thicknesses of the composite core. Assuming a termination of the OSM at the end of C5Cn.1n, the average accumulation rate for the whole succession is 9 cm/kyr in model 1, while it is 5 cm/kyr in model 2 when assuming that the top of C5Cn.2n was reached. Note that these are minimum estimates, because the top of the OSM in the cores is probably older than the top of the normal subchron. Inside the OBM, we notice a minimum rate of ~14 cm/kyr (model 1) versus ~2 cm/kyr (model 2) in the Kirchberg Fm (when the base of the KS is tied to the base of the reversed chron), and ~7 cm/kyr (model 1) versus ~4 cm/kyr (model 2) for the normal interval in the Grimmelfingen Fm (Fig. 6). The rates in the high quality cores Buttenwiesen and Hamlar-1 differ <20% from those calculated using the composite profile.

Accumulation rates in the northern area of the Molasse Basin are generally lower than those in the central and southern areas nearby the Alpine front, where subsidence rates and fluvial input were higher (Bachmann and Müller, 1992; Kuhlemann and Kempf, 2002). Estimated rates from OSM deposits that are comparable in age and lithofacies to the here studied sediments, but which partially originated near to the Alpine fans in the Swiss Molasse Basin, are <15 cm/kyr (Kempf et al., 1999) or up to ~30 cm/kyr (Kälin and Kempf, 2009). Our sedimentation rates appear relatively low for both models. The low rates could be a result of the paleogeographic situation of our boreholes in the distal part of the Molasse Basin, far away from the large Alpine fans, or could reflect some stratigraphic gaps.

Noticeably, the ages for the onset of freshwater sedimentation (base OSM) for correlation model 1 and 2 are close to each other, 16.47 and 16.72 Ma, respectively. We conclude that without additional reliable age data for the OBM and OMM, it is not possible to favor one over the other (Fig. 6).

5.3. Stratigraphic and climatic implications

Fig. 7 shows how the two proposed models would fit to the time scales and mammal biostratigraphic framework for the Molasse Basin. The age for the base of the Freshwater Molasse (OSM) in the study area is similar (model 1) or slightly older (model 2) than the age of the base OSM in the Swiss Molasse Basin as published by Reichenbacher et al. (2013). This is likely because the Upper Marine Molasse sea retreated later from Switzerland than from southern Germany (Kuhlemann and Kempf, 2002; Reichenbacher et al., 2005).

Our new data further reveal the presence of several, probably small hiatuses within the OBM deposits. Examples are the reverse part of the uppermost GS (missing in Hamlar-1 and Gundremmingen), and the absence of the lower KS in the boreholes Glött, Dillingen and Offingen. In addition, strong variations in the thickness of the KS occur. This implies a very dynamic environment with multiple variations in accommodation space during the infill of the Graupensand channel.

Species of the brackish bivalve *Rzehakia* are generally widespread in upper Ottnangian sediments of the entire Paratethys (Čtyroký, 1968). Considering the time range of *Rzehakia*, model 1 would propose that this brackish bivalve survived in the study area up to ~16.5 Ma (regional Karpatian stage), whereas for model 2 it would have existed at least up to ~17.2 Ma (top upper Ottnangian).

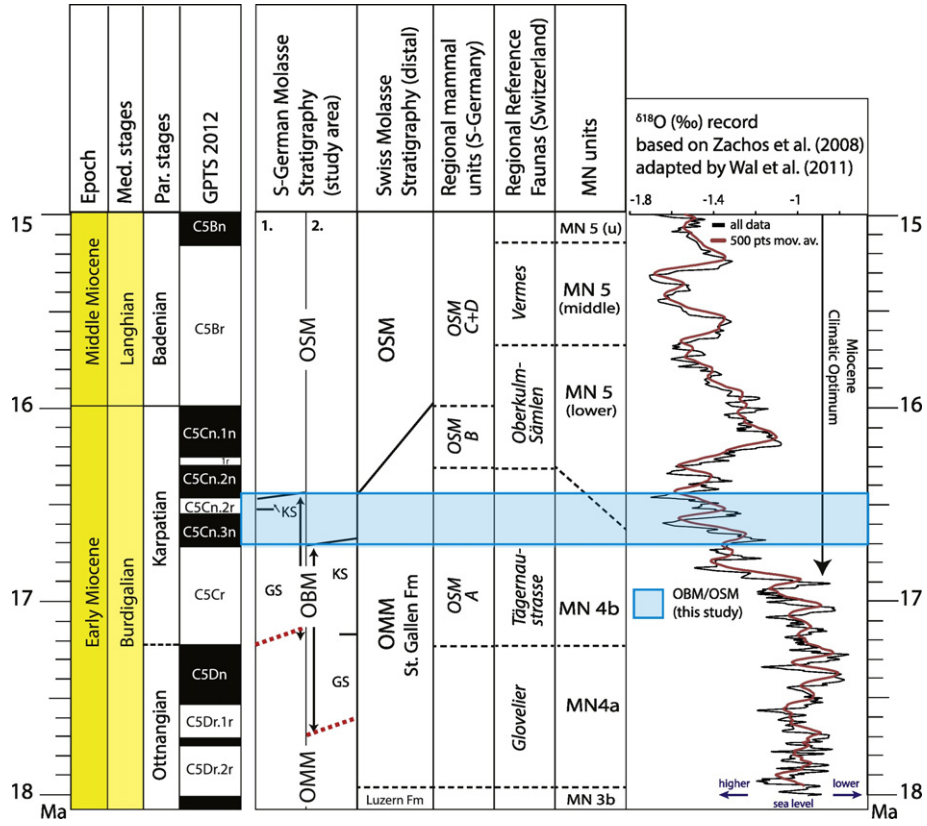

Fig. 7. Correlation of the proposed models 1 and 2 to the time scales and mammal biostratigraphic framework of the study area in the Molasse Basin. Time scales, fossil zones and abbreviations as in Fig. 2. The difference between the ages for the base of the Upper Freshwater Molasse (OSM) according to the two possible models is shaded in blue. The maximum ages for the base of the GS according to both age models are shown with red dashed lines. Time range of Miocene Climatic Optimum after Holbourn et al. (2015), oxygen isotope record after Zachos et al. (2008) and Wal et al. (2011). (For interpretation of the references to color in this figure legend, the reader is referred to the web version of this article.)

A comparison of our two models to the global climate curve derived from $\delta^{18}O$-isotope data (Wal et al., 2011) reveals that the final retreat of the sea occurred within the lower part of the Miocene Climatic Optimum (MCO), regardless which model is adopted. This implies that tectonics rather than climate change has controlled this significant change of the paleoenvironment in the NAFB. Furthermore, the transgression of the KS would have taken place during the MCO in case of model 1. Concerning model 2, we do not precisely know when within Chron C5Cr the KS transgression took place. The transgression could have been coincident with the onset of the MCO. The re-appearance of tropical fish in the KS, such as the ambassids (represented with species of *Dapalis*, see Reichenbacher et al., 2013), which nowadays are mainly found in tropical to subtropical areas of the Indo-Pacific, supports deposition within or at the beginning of the MCO.

5.4. Temporal implications on paleogeography

The Kirchberg Fm of the Upper Brackish Molasse (OBM) represents the last marine transgression in the S-German Molasse Basin (e.g., Lemcke, 1988), and the Upper Freshwater Molasse (OSM) marks the final retreat of the marine realm (e.g., Kuhlemann and Kempf, 2002). Our study confirms a younger age for the base of the OSM of at least 16.7 Ma, which is younger than proposed by Abdul Aziz et al. (2010). This has paleogeographic implications for the western S-German Molasse Basin during the late Burdigalian (Lower Miocene).

Fig. 8a represents the paleogeography in the central NAFB around 18.0 Ma during the OMM. The basin is well-connected to the western Mediterranean via the "Gulf of Lions" and "Gulf of Digne", and marine conditions prevail in Switzerland (St. Gallen Fm), SE Germany and Upper Austria (e.g., Sissingh, 2001). To the east, it remains connected to other parts of the Central Paratethys sea. Most material is sourced from the Alpine front, and some additional material derived from the northern margins (e.g., Kuhlemann and Kempf, 2002).

Subsequently, the paleogeography of the NAFB begins to change, the sea starts to retreat from the western S-German Molasse Basin, and the Graupensand channel incises along the northwestern basin margin bringing abundant material from the Palaeo-Main and the Bohemian Massif (Lemcke, 1985; Pippèrr and Reichenbacher, 2017). In the S-German Molasse Basin this might have started as early as 17.7 Ma according to correlation option 2, or around 17.2 Ma if correlation option 1 is followed. A stepwise retreat of the sea can be observed over the entire area of the Paratethys, which was most likely controlled by an interplay of several factors including an increase in clastic input by enhanced erosion along the Alpine front, decreased subsidence rates, global sea level fall and changes in precipitation (e.g., Kempf et al., 1999; Sissingh, 2001).

In the western S-German Molasse Basin, the last transgressive phase is marked by the deposition of the Kirchberg Fm (Fig. 8b). The transgression may not have reached the Austrian side east of the Bohemian Massif, since an uplifted block (the 'Amstetten Swell') might have impeded the passage south of the Bohemian Massif (Kuhlemann and Kempf, 2002). Shallow marine deposition continues solely in the westernmost parts of the North Alpine Foreland Basin (Swiss Molasse Basin).

At the onset of OSM deposition the drainages of the Swiss and S-German Molasse Basins are most likely fully separated from the eastern part of the Austrian Molasse Basin, because of the uplift of the Amstetten swell (Kapounek et al., 1965). The sea gradually retreats from the Swiss Molasse Basin and the entire NAFB becomes fully terrestrial. The Upper Austrian Molasse Basin east of the Bohemian Massif gets eventually re-connected to the Mediterranean via the Transtethyan corridor in Slovenia and becomes part of the Karpatian Sea of the Central Paratethys realm (e.g., Kováč et al., 2003).

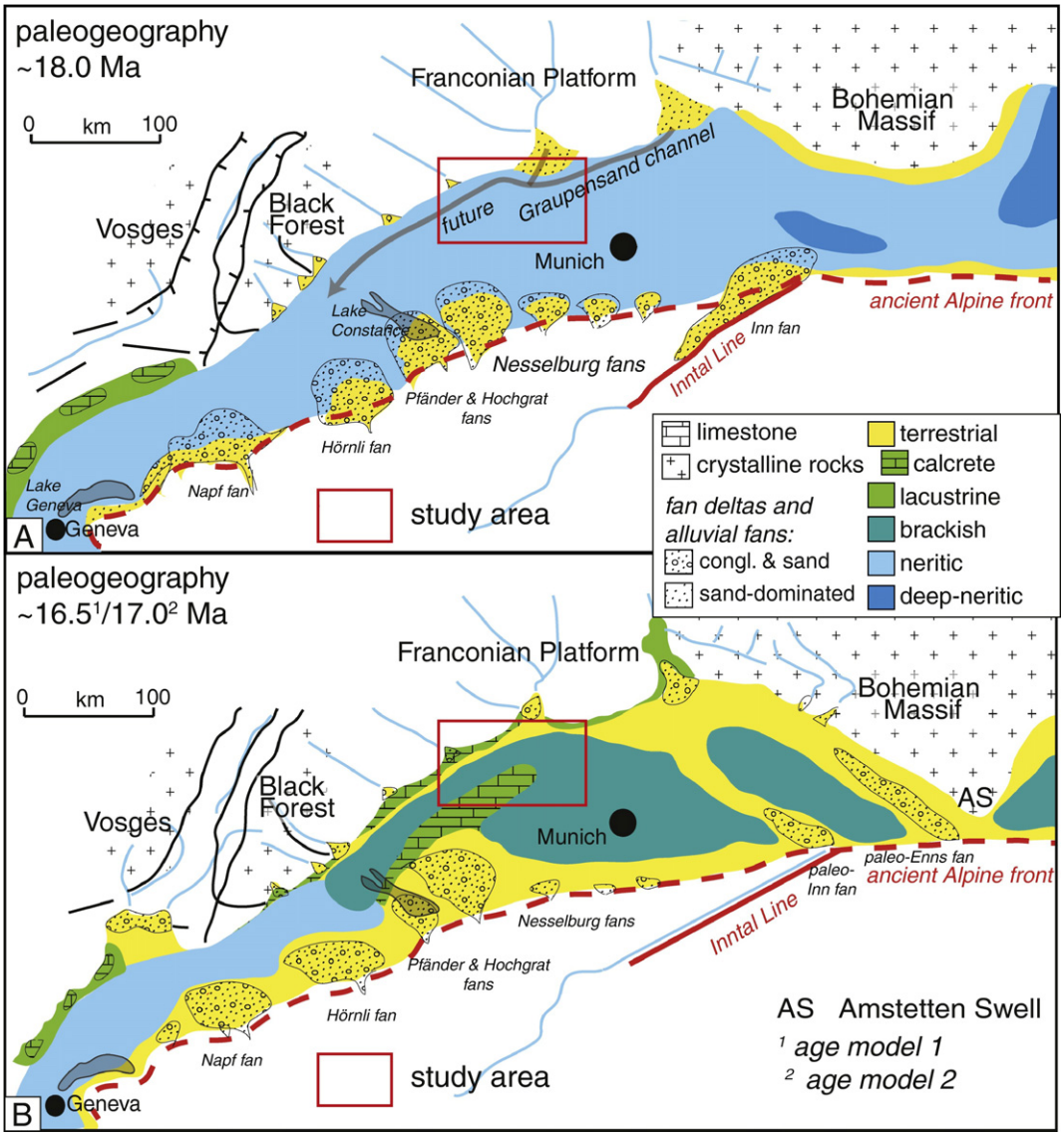

Fig. 8. Paleogeographic sketches of the North Alpine Foreland basin, modified after Kuhlemann and Kempf (2002) and Berger et al. (2005a), with an updated ages for the base OSM from this study. In (A) the location of the future Graupensand channel in the northern margin (according to Lemcke, 1988) is indicated with a brown overlay. See text for more details. (For interpretation of the references to color in this figure legend, the reader is referred to the web version of this article.)

6. Summary and conclusions

We performed a high resolution magnetostratigraphic study comprising >550 samples on eleven drill cores of the late Burdigalian succession of the S-German Molasse Basin in order to improve the age framework of the North Alpine Foreland Basin (NAFB) during the Early Miocene. The highest quality drill cores show a very consistent magnetostratigraphic pattern and were combined in a representative composite column. We propose two different age correlations to the GPTS. In model 1, we assume relatively constant accumulation rates and we correlate the polarity pattern to the interval C5Cr to C5Cn.1n, while in model 2, taking into account discontinuities, we correlate the pattern to the interval C5Dr.1r to C5Cn.2n. The final retreat of the sea and onset of Upper Freshwater Molasse (OSM) deposition would be at ~16.5 Ma in model 1, and at ~16.7 Ma in model 2.

Our new results substantially back up the age data of Reichenbacher et al. (2013) and date the end of marine conditions in the western S-German Basin in the late Burdigalian. Both age models confirm a relatively young age for the base of the OSM younger than 16.7 Ma, which is at least 0.7 Myr younger than in Abdul Aziz et al. (2010). The revised time frame has served as the basis for a new time calibration of the paleogeographic and paleoenvironmental reconstructions of the NAFB and the Paratethys domain during the late Early Miocene. Regardless which age model is used, the onset of OSM does not seem to be triggered by a climate event, but the sedimentation of the transgressive Kirchberg Fm apparently is related to the Miocene Climate Optimum.

We suggest that obtaining high resolution magnetostratigraphic data in the underlying Upper Marine Molasse (OMM) is the next logical step forward to finally solve the Early Miocene chronostratigraphy of the NAFB, and to further improve the paleogeographic reconstructions of the Western and Central Paratethys. Moreover, a resolved Early Miocene chronostratigraphy would serve as a strong basis to further identify the drivers (climate or tectonics) causing the main paleoenvironmental changes in the area.

Acknowledgements

Special thanks go to the people of the Bavarian Environment Agency (LfU) in Hof for their help during the sampling campaign. The new set of Molasse boreholes only exists because of the financial support given by the European Fund for Regional Development (EFRE) and the LfU. This research was financially supported through the Netherlands

Geosciences Foundation (ALW) with funding from the Netherlands Organization for Scientific Research (NWO) by VICI grant 865.10.011 of WK. We are also grateful for the constructive feedback which we received from Imre Magyar, Oliver Kempf and Patrick Grunert.

Appendix A. Supplementary data

Supplementary data associated with this article can be found in the online version, at doi:10.1016/j.gloplacha.2017.02.002. This data includes the gps coordinates of the sample locations described in this article.

References

Abdul Aziz, H., Böhme, M., Rocholl, A., Zwing, A., Prieto, J., Wijbrans, J.R., Heissig, K., Bachtadse, V., 2008. Integrated stratigraphy and $^{40}Ar/^{39}Ar$ chronology of the Early to Middle Miocene Upper Freshwater Molasse in eastern Bavaria (Germany). Int. J. Earth Sci. 97, 115–134.

Abdul Aziz, H., Böhme, M., Rocholl, A., Prieto, J., Wijbrans, J.R., Bachtadse, V., Ulbig, A., 2010. Integrated stratigraphy and $^{40}Ar/^{39}Ar$ chronology of the Early to Middle Miocene Upper Freshwater Molasse in western Bavaria (Germany). Int. J. Earth Sci. 99, 1859–1886.

Bachmann, G.H., Müller, M., 1992. Sedimentary and structural evolution of the German Molasse Basin. Eclogae Geol. Helv. 85, 519–530.

Berger, J.-P., Reichenbacher, B., Becker, D., Grimm, M., Grimm, K., Picot, L., Storni, A., Pirkenseer, C., Derer, C., Schaefer, A., 2005a. Paleogeography of the Upper Rhine Graben (URG) and the Swiss Molasse Basin (SMB) from Eocene to Pliocene. Int. J. Earth Sci. 94, 697–710.

Berger, J.P., Reichenbacher, B., Becker, D., Grimm, M., Grimm, K., Picot, L., Storni, A., Pirkenseer, C., Schaefer, A., 2005b. Eocene-Pliocene time scale and stratigraphy of the Upper Rhine Graben (URG) and the Swiss Molasse Basin (SMB). Int. J. Earth Sci. 94, 711–731.

Büchi, U.P., Schlanke, S., 1977. Zur Paläogeographie der Schweizerischen Molasse. Erdöl-Erdgas-Z. 93, 57–69.

Cicha, I., Rögl, F., Rupp, C., Ctyroka, J., 1998. Oligocene-Miocene foraminifera of the Central Paratethys. Abh. Senckenb. Naturforsch. Ges. 549, 1–325.

Čtyroký, P., 1968. The correlation of Rzehakia (Oncophora) series (Miocene) in Eurasia. Palaeogeogr. Palaeoclimatol. Palaeoecol. 4, 257–270.

Daxner-Höck, G., 1998. Säugetiere (Mammalia) aus dem Karpat des Korneuburger Beckens 3. Rodentia und Carnivora. Beitr. Paläontol. 23, 367–407.

Doppler, G., 1989. Zur Stratigraphie der nördlichen Vorlandmolasse in Bayerisch-Schwaben. Geologica Bavarica 94, 83–133.

Doppler, G., Heissig, K., Reichenbacher, B., 2005. Die Gliederung des Tertiärs im süddeutschen Molassebecken. Newsl. Stratigr. 41, 359–375.

Dupont-Nivet, G., Krijgsman, W., 2012. Magnetostratigraphic methods and applications. In: Busby, C., Azor, A. (Eds.), Recent Advances in Tectonics of Sedimentary Basins. Blackwell Publishing Ltd., pp. 80–94.

Fisher, R., 1953. Dispersion on a sphere. Proc. Roy. Soc. London A217, 295–305.

Frieling, D., Aehnelt, M., Scholz, H., Reichenbacher, B., 2009. Sequence stratigraphy of an alluvial fan-delta in the Upper Marine Molasse (Pfänder area, late Burdigalian, Miocene). Z. Dtsch. Ges. Geowiss. 160, 333–357.

Gierl, C., Reichenbacher, B., 2015. A new fossil genus of Gobiiformes from the Miocene characterized by a mosaic set of characters. Copeia 103 (4), 792–805.

Grunert, P., Soliman, A., Ćorić, S., Scholger, R., Harzhauser, M., Piller, W.E., 2010. Stratigraphic re-evaluation of the stratotype for the regional Ottnangian stage (Central Paratethys, middle Burdigalian). Newsl. Stratigr. 44, 1–16.

Grunert, P., Soliman, A., Coric, S., Roetzel, R., Harzhauser, M., Piller, W.E., 2012. Facies development along the tide-influenced shelf of the Burdigalian Seaway: an example from the Ottnangian stratotype (Early Miocene, middle Burdigalian). Mar. Micropaleontol. 84-85, 14–36.

Grunert, P., Hinsch, R., Sachsenhofer, R.F., Bechtel, A., Ćorić, S., Harzhauser, M., Piller, W.E., Sperl, H., 2013. Early Burdigalian infill of the Puchkirchen Trough (North Alpine Foreland Basin, Central Paratethys): facies development and sequence stratigraphy. Mar. Pet. Geol. 39, 164–186.

Grunert, P., Auer, G., Harzhauser, M., Piller, W.E., 2015. Stratigraphic constraints for the upper Oligocene to lower Miocene Puchkirchen Group (North Alpine Foreland Basin, Central Paratethys). Newsl. Stratigr. 48, 111–133.

Hardenbol, J., Thierry, J., Farley, M.B., Jacquin, T., de Graciansky, P., Vail, P.R., 1998. Mesozoic and Cenozoic sequence chronostratigraphic framework of European basins. SEPM Spec. Publ. 60, 3–13.

Heslop, D., Dekkers, M., Kruiver, P., van Oorschot, I., 2002. Analysis of isothermal remanent magnetization acquisition curves using the expectation-maximization algorithm. Geophys. J. Int. 148, 58–64.

Hilgen, F.J., Lourens, L.J., Van Dam, J.A., 2012. The Neogene period. The Geologic Time Scale 2012. Vol. 2, pp. 923–978.

Hinsch, R., 2008. New insights into the Oligocene to Miocene geological evolution of the Molasse Basin of Austria. Oil Gas Eur. Mag. 34, 138–143.

Hirt, A.M., Gerhring, A.U., 1991. Thermal alteration of the magnetic mineralogy in ferruginous rocks. J. Geophys. Res. 96, 9947–9953.

Holbourn, A., Kuhnt, W., Kochhann, K.G.D., Andersen, N., Meier, K.J.S., 2015. Global perturbation of the carbon cycle at the onset of the Miocene Climatic Optimum. Geology 43, 123–126.

Jin, J., Aigner, T., Luterbacher, H.P., Bachmann, G.H., Müller, M., 1995. Sequence stratigraphy and depositional history in the south-eastern German Molasse Basin. Mar. Pet. Geol. 12, 929–940.

Jost, J., Kälin, D., Börner, S., Vasilyan, D., Lawver, D., Reichenbacher, B., 2015. Vertebrate microfossils from the Upper Freshwater Molasse in the Swiss Molasse Basin: implications for the evolution of the North Alpine Foreland Basin during the Miocene Climate Optimum. Palaeogeogr. Palaeoclimatol. Palaeoecol. 426, 22–33.

Kälin, D., Kempf, O., 2009. High-resolution stratigraphy from the continental record of the Middle Miocene Northern Alpine Foreland Basin of Switzerland. N. Jb. Geol. Paläont. (Abh.) 254, 177–235.

Kapounek, J., Kröll, A., Papp, A., Turnovsky, K., 1965. Die Verbreitungvon Oligozän, Unter- und Mittelmiozän in Niederösterreich. Erdoel-Erdgas-Z. 81, 109–115.

Kempf, O., Matter, A., Burbank, D.W., Mange, M., 1999. Depositional and structural evolution of a foreland basin margin in a magnetostratigraphic framework: the eastern Swiss Molasse Basin. Int. J. Earth Sci. 88, 253–275.

Kiderlen, H., 1931. Beiträge zur Stratigraphie und Paläogeographie des süddeutschen Tertiärs. Neues Jahrbuch für Mineralogie, Geologie und Paläontologie, Abteilung B, Beilageband. Vol. 66 pp. 215–384.

Kirscher, U., Prieto, J., Bachtadse, V., Aziz, H.A., Doppler, G., Hagmaier, M., Böhme, M., 2016. A biochronologic tie-point for the base of the Tortonian stage in European terrestrial settings: magnetostratigraphy of the topmost Upper Freshwater Molasse sediments of the North Alpine Foreland Basin in Bavaria (Germany). Newsl. Stratigr. 49, 445–467.

Kirschvink, J.L., 1980. The least-square line and plane and the analysis of paleomagnetic data. Geophys. J. R. Astron. Soc. 62, 699–718.

Kováč, M., Andreyeva-Grigorovich, A.S., Brzobohatý, R., Fodor, L., Harzhauser, M., Oszczypko, N., Pavelić, D., Rögl, F., Saftić, B., Sliva, L., Stráník, Z., 2003. Karpatian paleogeography, tectonics and eustatic changes. In: Brzobohatý, R., Cicha, I., Kováč, M., Rögl, F. (Eds.), The Karpatian: a Lower Miocene Stage of the Central Paratethys. Masaryk University, Brno, pp. 49–72.

Kranz, W., 1904. Stratigraphie und Alter der Ablagerungen bei Unter- und Oberkirchberg, südlich Ulm a. D. Centralblatt für Mineralogie, Geologie, Paläontologie 1904. Vol. 481–502 pp. 528-540–545-566.

Krása, D., Petersen, K., Petersen, N., 2007. Variable field translation balance. Encyclopedia of earth sciences series, 977–979. In: Gubbins, D., Herrero-Bervera, E. (Eds.), Encyclopedia of Geomagnetism and Paleomagnetism.

Kruiver, P.P., Dekkers, M.J., Heslop, D., 2001. Quantification of magnetic coercivity components by the analysis of acquisition curves of isothermal remanent magnetisation. Earth Planet. Sci. Lett. 189, 0–7.

Kuhlemann, J., Kempf, O., 2002. Post-Eocene evolution of the North Alpine Foreland Basin and its response to Alpine tectonics. Sediment. Geol. 152, 45–78.

Lemcke, K., 1985. Flußfracht von Ur-Main und Ur-Naab in der Schweiz und im deutschen Molassebecken. Bull. der Vereinigung Schweizerischer Petroleumgeologen und Petroleumingenieure 51, 13–21.

Lemcke, K., 1988. Geologie von Bayern I: Das bayerische Alpenvorland vor der Eiszeit - Erdgeschichte, Bau, Bodenschätze. Schweizerbart, Stuttgart.

Lemcke, K., Engelhardt, W.v., Füchtbauer, H., 1953. Geologische und sedimentologische Untersuchungen im Westteil der ungefalteten Molasse des süddeutschen Alpenvorlandes. Beihefte zum Geologischen Jahrbuch. Vol. 11, pp. 1–110.

Moos, A., 1926. Zur Bildung von Ablagerungen mit Landsäugetierresten in der süddeutschen Molasse. Geol. Rundsch. 17, 8–21.

Passier, H.F., de Lange, G.J., Dekkers, M.J., 2001. Magnetic properties and geochemistry of the active oxidation front and the youngest sapropel in the eastern Mediterranean Sea. Geophys. J. Int. 145, 604–614.

Piller, W.E., Harzhauser, M., Mandic, O., 2007. Miocene Central Paratethys stratigraphy - current status and future directions. Stratigraphy 4, 151–168.

Pippèrr, M., 2011. Characterisation of Ottnangian (middle Burdigalian) palaeoenvironments in the North Alpine Foreland Basin using benthic foraminifera - a review of the Upper Marine Molasse of southern Germany. Mar. Micropaleontol. 79, 80–99.

Pippèrr, M., Reichenbacher, B., 2017. Late Early Miocene palaeoenvironmental changes in the North Alpine Foreland Basin. Palaeogeogr. Palaeoclimatol. Palaeoecol. 468, 485–502.

Pippèrr, M., Reichenbacher, B., Witt, W., Rocholl, A., 2007. The middle and Upper Ottnangian of the Simssee area (SE Germany): micropalaeontology, biostratigraphy and chronostratigraphy. N. Jb. Geol. Paläont. (Abh.) 245, 353–378.

Pippèrr, M., Reichenbacher, B., Doppler, G., Hagmaier, M., Jung, D., 2016. The northern coast of the Ottnangian (middle Burdigalian, early Miocene) Molasse Sea in Germany: sediments, foraminiferal assemblages and biostratigraphy. Int. J. Earth Sci. 105, 1055–1085.

Prieto, J., Böhme, M., Maurer, H., Heissig, K., Abdul Aziz, H., 2009. Sedimentology, biostratigraphy and environments of the Untere Fluviatile Serie (Lower and Middle Miocene) in the central part of the North Alpine Foreland Basin - implications for basin evolution. Int. J. Earth Sci. 98, 1767–1791.

Reichenbacher, B., 1989. Feinstratigraphische Gliederung der Kirchberger Schichten (Unter-Miozän) an der Typuslokalität Illerkirchberg bei Ulm. Geol. Bavarica 94, 135–177.

Reichenbacher, B., 1999. Preliminary otolith-zonation in continental tertiary deposits of the Paratethys and adjacent areas. N. Jb. Geol. Paläont. (Abh.) 214, 375–390.

Reichenbacher, B., Böttcher, R., Bracher, H., Doppler, G., Engelhardt, W.v., Gregor, H.-J., Heissig, K., Heizmann, E.P.J., Hofmann, F., Kälin, D., Lemcke, K., Luterbacher, H., Martini, E., Pfeil, F., Reiff, W., Schreiner, A., Steininger, F.F., 1998. Graupensandrinne – Ries-Impakt: Zur Stratigraphie der Grimmelfinger Schichten, Kirchberger Schichten und Oberen Süßwassermolasse (nördliche Vorlandmolasse, Süddeutschland). Z. Dtsch. Geol. Ges. 149, 127–161.

Reichenbacher, B., Kälin, D., Jost, J., 2005. A fourth St. Gallen formation cycle (?) in the Karpatian upper Marine Molasse of central Switzerland. Facies 51, 160–172.
Reichenbacher, B., Krijgsman, W., Lataster, Y., Pippèrr, M., Van Baak, C.G.C., Chang, L., Kälin, D., Jost, J., Doppler, G., Jung, D., Prieto, J., Abdul Aziz, H., Böhme, M., Garnish, J., Kirscher, U., Bachtadse, V., 2013. A new magnetostratigraphic framework for the lower Miocene (Burdigalian/Ottnangian, Karpatian) in the North Alpine Foreland Basin. Swiss J. Geosci. 106, 309–334.
Sach, V.J., Heizmann, E.P.J., 2001. Stratigraphie und Säugetierfaunen der Brackwassermolasse in der Umgebung von Ulm (Südwestdeutschland). Stuttg. Beitr. Naturkunde B 310, 1–95.
Schlickum, W.R., 1963. Die Molluskenfauna der Süßbrackwassermolasse von Ober- und Unterkirchberg. Arch. Molluskenkd. 92, 1–10.
Schlunegger, F., Burbank, D.W., Matter, A., Engesser, B., Mödden, C., 1996. Magnetostratigraphic calibration of the Oligocence to Middle Miocene (30–15 Ma) mammal biozones and depositional sequences of the Swiss Molasse Basin. Eclogae Geol. Helv. 89, 753–788.
Senes, J., 1973. Die Sedimentationsräume und die Schichtengruppen der zentralen Paratethys im Ottnangien. In: Papp, A., Rögl, F., Seneš, J. (Eds.), M2 – Ottnangien. Die Innviertler, Salgótarjáner, Bántapusztaer Schichtengruppe und die Rzehakia Formation. Chronostratigraphie und Neostratotypen, Miozän der Zentralen Paratethys. Vol. 3, pp. 45–53.
Sissingh, W., 1997. Tectonostratigraphy of the North Alpine Foreland Basin: correlation of Tertiary depositional cycles and orogenic phases. Tectonophysics 282, 223–256.
Sissingh, W., 2001. Tectonostratigraphy of the West Alpine Foreland: correlation of tertiary sedimentary sequences, changes in eustatic sea-level and stress regimes. Tectonophysics 333, 361–400.
Steininger, F., Rögl, F., Martini, E., 1976. Current Oligocene/Miocene biostratigraphic concept of the Central Paratethys (Middle Europe). Newsl. Stratigr. 4, 174–202.
Stephenson, A., Snowball, I.F., 2001. A large gyromagnetic effect in greigite. Geophys. J. Int. 145, 570–575.
Wack, M., Gilder, S., 2012. The SushiBar: an automated system for paleomagnetic investigations. Geochem. Geophys. Geosyst. 13, 1–24.
Wal van de, R.S.W., Boer de, B., Lourens, L.J., Köhler, P., Bintanja, R., 2011. Reconstruction of a continuous high-resolution CO2 record over the past 20 million years. Clim. Past 7, 1459–1469.
Wenger, W.F., 1987. Die Foraminiferen des Miozäns der bayerischen Molasse und ihre stratigraphische sowie paläogeographische Auswertung. Zitteliana 16, 173–340.
Zachos, J.C., Dickens, G.R., Zeebe, R.E., 2008. An early Cenozoic perspective on greenhouse warming and carbon-cycle dynamics. Nature 451, 279–283.
Zijderveld, J., 1967. A. C. demagnetization of rocks: analysis of results. In: Collinson, D.W., Creer, K.M., Runcorn, S.K. (Eds.), Methods in Paleomagnetism. Elsevier, Amsterdam, pp. 254–286.
Zweigel, J., Aigner, T., Luterbacher, H., 1998. Eustatic versus tectonic controls on Alpine foreland basin fill: sequence stratigraphy and subsidence analysis in the SE German Molasse. In: Mascle, A., Puigdefàbregas, C., Luterbacher, H.P., Fernàndez, M. (Eds.), Cenozoic Foreland Basins of Western Europe. Geol. London Soc. Spec. Publ. Vol. 134. Geol. Soc. London, pp. 299–323.